marineFoam: Porous Media Modelling for Flow Through Fish Farm Cages

Dr Tom Scanlon BEng PhD CEng MIMechE

www.mts-cfd.com

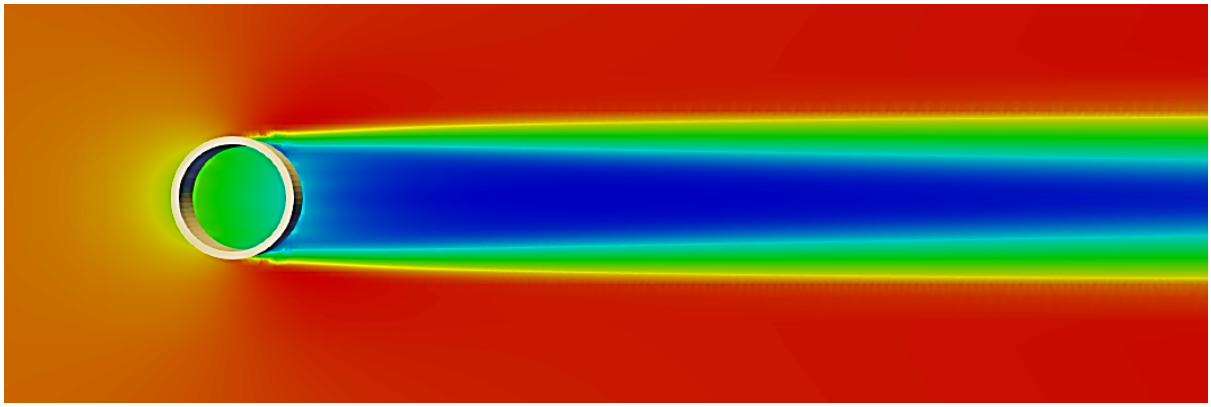

Abstract

marineFoam is a new computational fluid dynamics (CFD) tool aimed at modelling the flow around and through salmon farm cages including dispersion of anti-parasitic chemicals used during bath treatments to counteract sea lice. The computational model has been developed within the framework of the open-source, finite volume CFD code OpenFOAM and is designed to be used either as a high-fidelity, stand-alone code or as a complementary tool to inform and improve the lower-order bath treatment models currently promoted by SEPA. Porous media have now been introduced into the *marineFoam* code in order to represent the flow through and around the nets that form typical farmed salmon sea cages. Cage skin friction and form drag are characterised using porous resistance coefficients determined from published experimental data. Results show that the open-source *marineFoam* code performs well when compared with physical experiments and state-of-the-art numerical models currently found in the scientific literature.

1. Introduction

The numerical modelling of the flow through and around salmon farm cages is important for the characterisation of the local sea environment regarding the transport of anti-sea-lice chemicals following bath treatments, sea bed particle resuspension, the transport of organic material emanating from the farm and oxygen depletion in multiple cage systems. However, the length scales involved in computational modelling of fish farms range from millimetres to

kilometres as the flow traverses salmon sea cages with net twine diameters typically around 3 mm contained within a tidal system covering several kilometres. Computational limitations mean that the smallest length scales require to be modelled as porous media and the salmon cage is normally represented as a continuous physical zone with momentum sink terms to represent the flow losses across the net surface. Patursson *et al* [1-2] and Winthereig-Rusmussen [3] have performed experimental and numerical work to assess the forces acting on sections of cage netting with empirically-derived porous media resistance coefficients. The resistance coefficients have been implemented into CFD models using the commercial code Fluent and the results show satisfactory agreement between experiment and numerical models. Chen and Christensen [4] used an older version of the OpenFOAM CFD code to model the flow through net cage sections at various angles of attack in addition to considering circular cages. Their study did not include a turbulence model and, although general results proved reasonable in comparison with experimental work, differences did exist between their numerical output and those of Patursson et al [1-2]. Bi and Xu [5] once again employed the commercial CFD code Fluent to perform numerical, porous media studies of flow across an 8-cage, full-scale fish farm. Their results highlighted the differences in the predicted flow-field for various cage depths and degrees of net bio-fouling when compared with the analytical solutions of Loland [6].

The work presented in this document highlights the development of an open-source CFD code (*marineFoam* [7]) for the analysis of flow in the vicinity of porous media derived fish cages including for the effects of turbulence across planar and circular nets and culminates in the study of a full-scale marine farm.

2. Porous Media in *marineFoam*

The pressure drop due to flow through an isotropic porous medium may be described using the Darcy-Forchheimer law [8]:

$$\frac{\partial P}{\partial x} = \frac{\mu}{\kappa_1} U + \frac{\rho}{\kappa_2} U^2 \tag{1}$$

where P [Pa] is the fluid pressure, x [m] the distance through the porous medium, μ [Pa.s] the dynamic viscosity, ρ [kg/ m^3] the fluid density, U [m/s] the fluid velocity, and κ_1 [m^2] and κ_2 [m] represent the resistivity of the porous medium and are known, respectively, as the *intrinsic* and *inertial* permeabilities.

It is conventional to represent the porous media properties not by permeabilities but rather as flow resistivity terms such that $r = \frac{\mu}{\kappa_1}$ [Pa.s/ m^2] is the *intrinsic* flow resistivity and $f = \frac{\rho}{\kappa_2}$ [Pa/ m] the *inertial* resistivity. The inertial resistivity may be considered as that due to *form* (*pressure*) *drag* while the intrinsic resistance is that due to *skin-friction drag*. This yields the Darcy-Forchheimer law given as:

$$\frac{\partial P}{\partial x} = rU + fU^2 \tag{2}$$

The porous pressure drop may be modelled by modifying the standard Navier-Stokes equations by adding a sink term:

$$\frac{\partial}{\partial t}(\rho u_i) + \frac{\partial}{\partial x_i}\left(\rho u_i u_j\right) = -\frac{\partial P}{\partial x} + \frac{\partial \tau_{ij}}{\partial x_i} + S_i \tag{3}$$

S_i is the porous sink term defined using the Darcy-Forchheimer law and written as:

$$S_i = -\left(r u_i + f\left|u_{ij}\right|u_i\right) \tag{4}$$

and τ_{ij} is the viscous stress tensor given by:

$$\tau_{ij} = \mu\left(\frac{\partial u_i}{\partial x_j} + \frac{\partial u_j}{\partial x_i}\right) \tag{5}$$

The sink term is coded in *marineFoam* as:

$$S_i = -\left(\mu D + \frac{1}{2}\rho\left|u_{ij}\right|F\right)u_i \tag{6}$$

Where D and F are the Darcy and Forchheimer coefficients, respectively. This dictates that the coefficients, as employed in *marineFoam*, are defined as follows:

$$D = r/\mu \quad [\mathrm{m}^{-2}] \tag{7}$$

and

$$F = 2f/\rho \quad [\mathrm{m}^{-1}] \tag{8}$$

In cases where the flow impinges on the porous material at a non-perpendicular angle of attack the Darcy and Forchheimer coefficients are resolved into their normal and tangential components according to the flow angle α shown in Figure 1 and the transformation matrix (simplified for 2D) shown in equation 9.

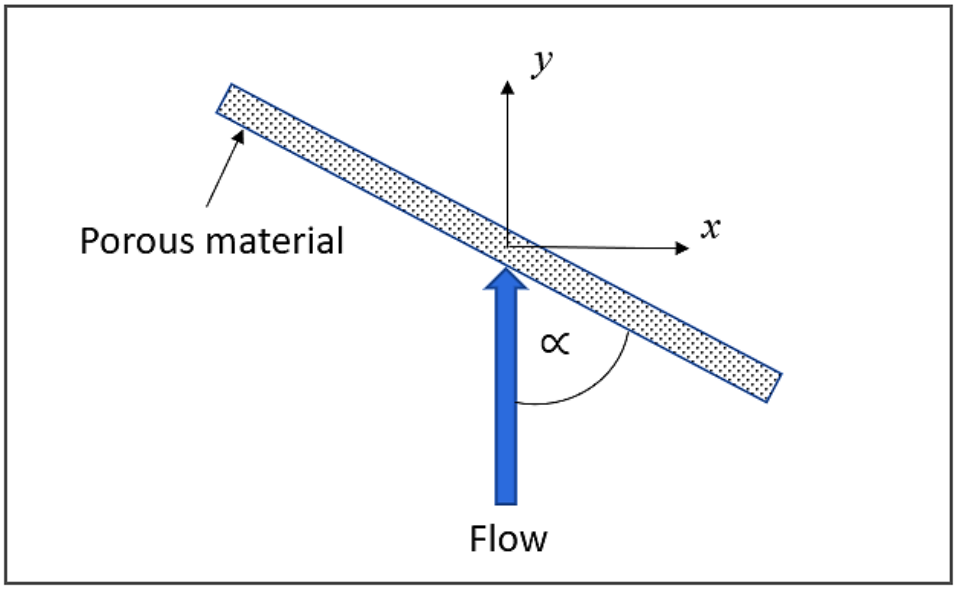

Figure 1 *Flow angle of attack*

$$\begin{bmatrix} cos \propto & \sin \propto \\ -sin \propto & cos \propto \end{bmatrix} \tag{9}$$

The modified Navier-Stokes equations may then be solved within *marineFoam* in conjunction with an appropriate turbulence model. In this document, the standard k-epsilon model has been applied for turbulence closure.

3. Code Validation

The implementation of porous media in *marineFoam* has been validated using a simple geometry test case. This case consists of 3 cubic sections with slip walls, each of side length 1 m with the middle section being of isotropic porous medium, as shown in Figure 2.

This case considers the flow of air with a density $\rho = 1.225$ kg/m^3, dynamic viscosity $\mu = 1.789 \times 10^{-5}$ kg/ ms (producing a value of kinematic viscosity $\upsilon = 1.46 \times 10^{-5}$ m^2/s) and a velocity of 2 m/s. The middle section consists of isotropic porous material with porous properties of inertial resistivity f =1 Pa/m and intrinsic resistivity r = 1 Pa.s/m^2. Converting the resistivities into their respective Darcy and Forchheimer coefficients using equations 7 and 8 produces values of D = 55897 m^{-2} and F = 1.633 m^{-1}. The pressure drop resulting should be that calculated using equation 2:

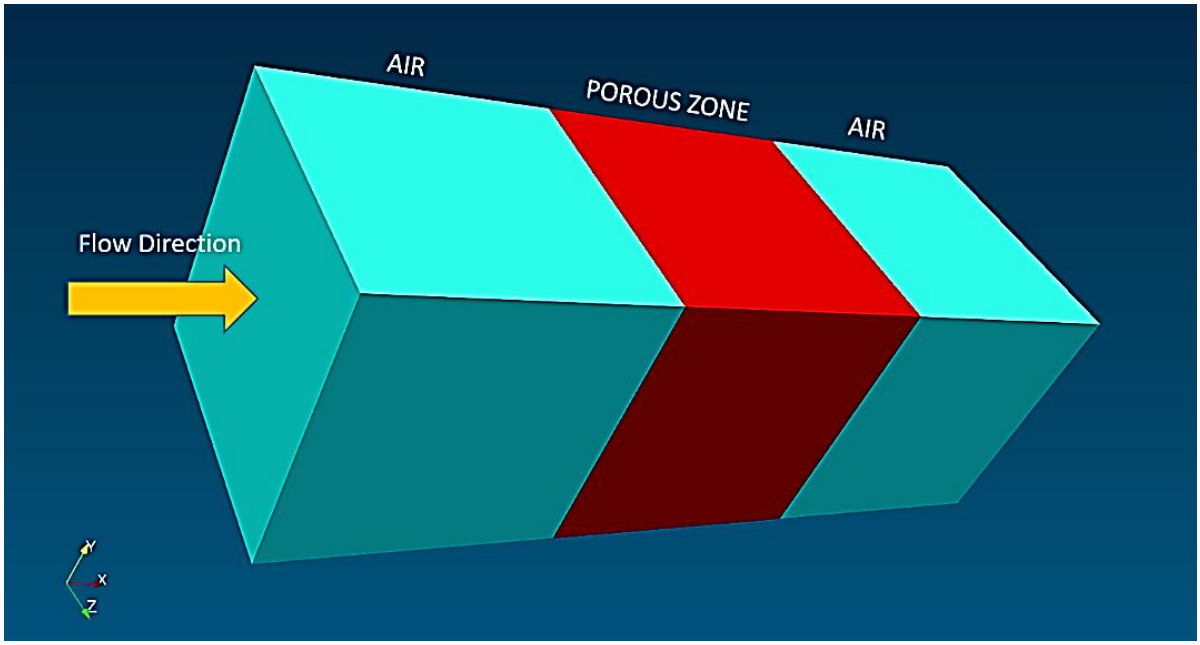

Figure 2 *Geometry for validation of porous media in marineFoam.*

$$\frac{\Delta P}{\Delta x} = rU + fU^2 \tag{9}$$

$$\Delta P = \Delta x \times (rU + fU^2) = 1 \times (1 \times 2 + 1 \times 2^2) = 6\ Pa \tag{10}$$

Figure 3 shows the resulting pressure distribution through the domain and Figure 4 shows a plot of pressure with distance.

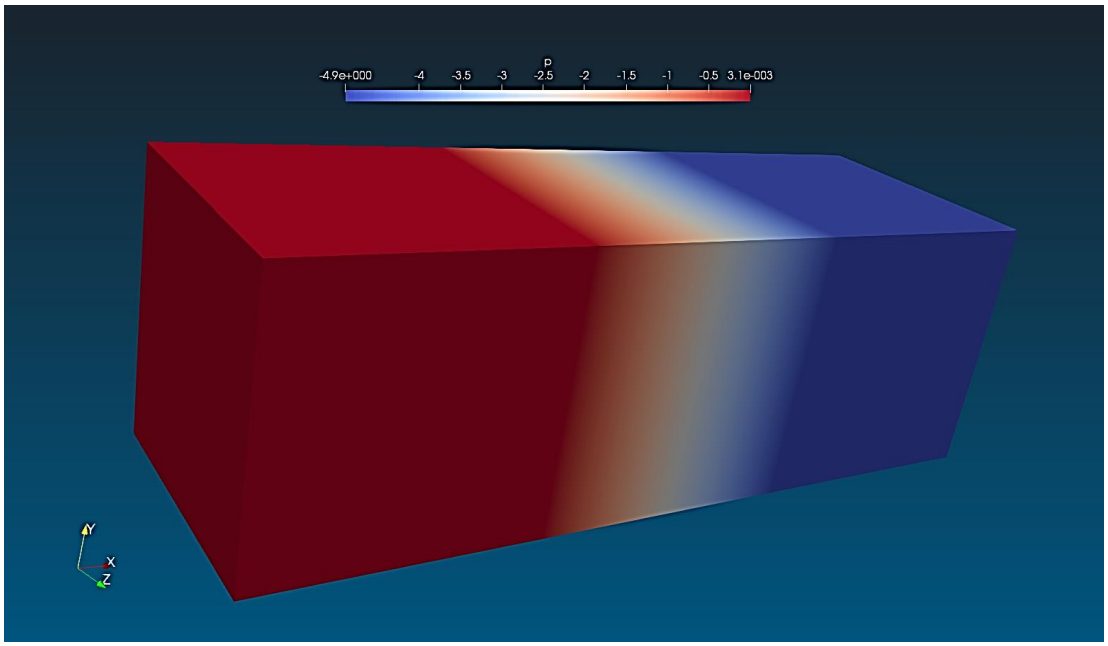

Figure 3 *Pressure distribution through the computational domain*

From figures 3 and 4 it is evident that the maximum pressure magnitude at the outlet is 4.9, however, as all OpenFOAM incompressible codes solve for P/ρ we need to multiply the value of 4.9 by the air density 1.225 kg/ m^3 to produce an outlet pressure magnitude of 6.002 Pa as expected from equation 10.

This test case highlights that the coding for porous media has been correctly implemented for any *marineFoam* application.

Figure 4 *Line plot of pressure versus distance through the computational domain.*

4. *marineFoam* Porous Media: Further Test Cases

Following the work of Chen and Christensen [4] two case studies are considered. The first concerns water flow across a planar net at various flow speeds and angles of attack and the determination of the forces acting on the net. The second considers flow through a circular cage net at different flow speeds. In the first case experimental tow tank work has been carried out by Patursson [1] and the second case by Zhan *et al* [9]. The CFD results of Chen and Christensen [4] and Patursson [2] are now compared with those of *marineFoam*. The porous resistance coefficients are detailed in the paper of Chen and Christensen [4] and are identical to those used for the *marineFoam* study.

The experimental set-up for the planar net case is shown in figure 5

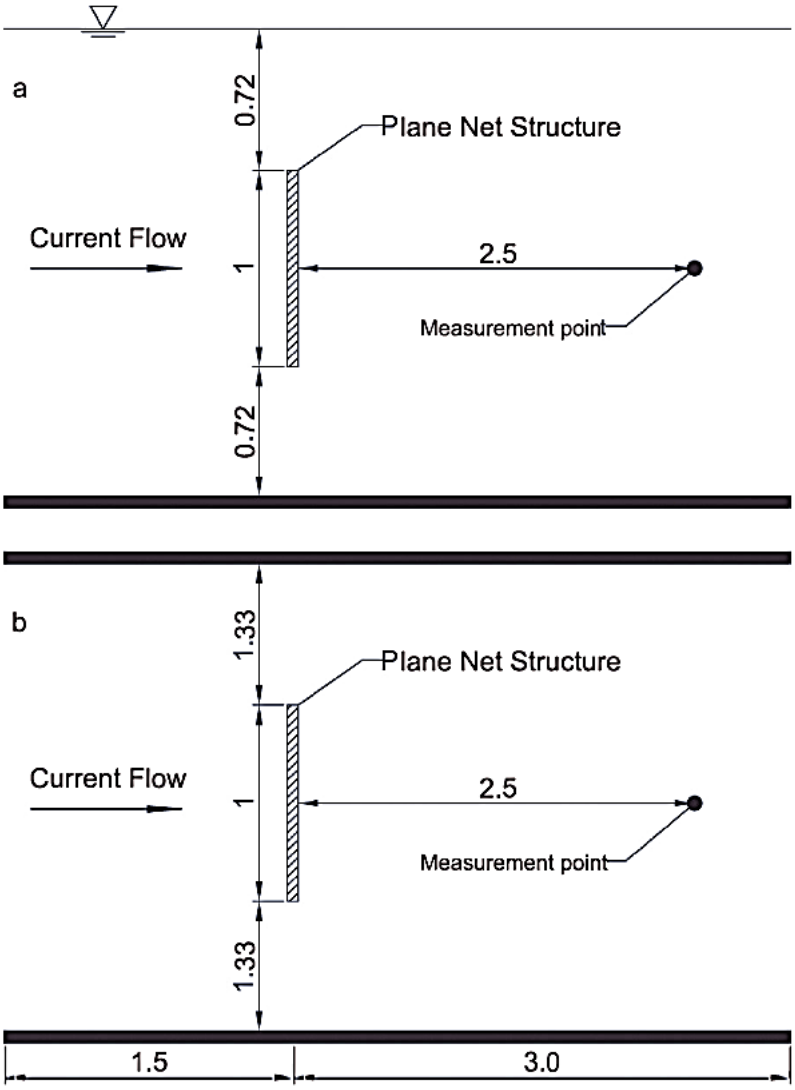

Figure 5 *Planar net configuration in the tow tank experiment of Patursson [1] (2008).*

Figure 6 compares the *marineFoam* porous media and Chen and Christensen [4] velocity contour plots at various angles of attack α for a flow speed of 0.5 m/s.

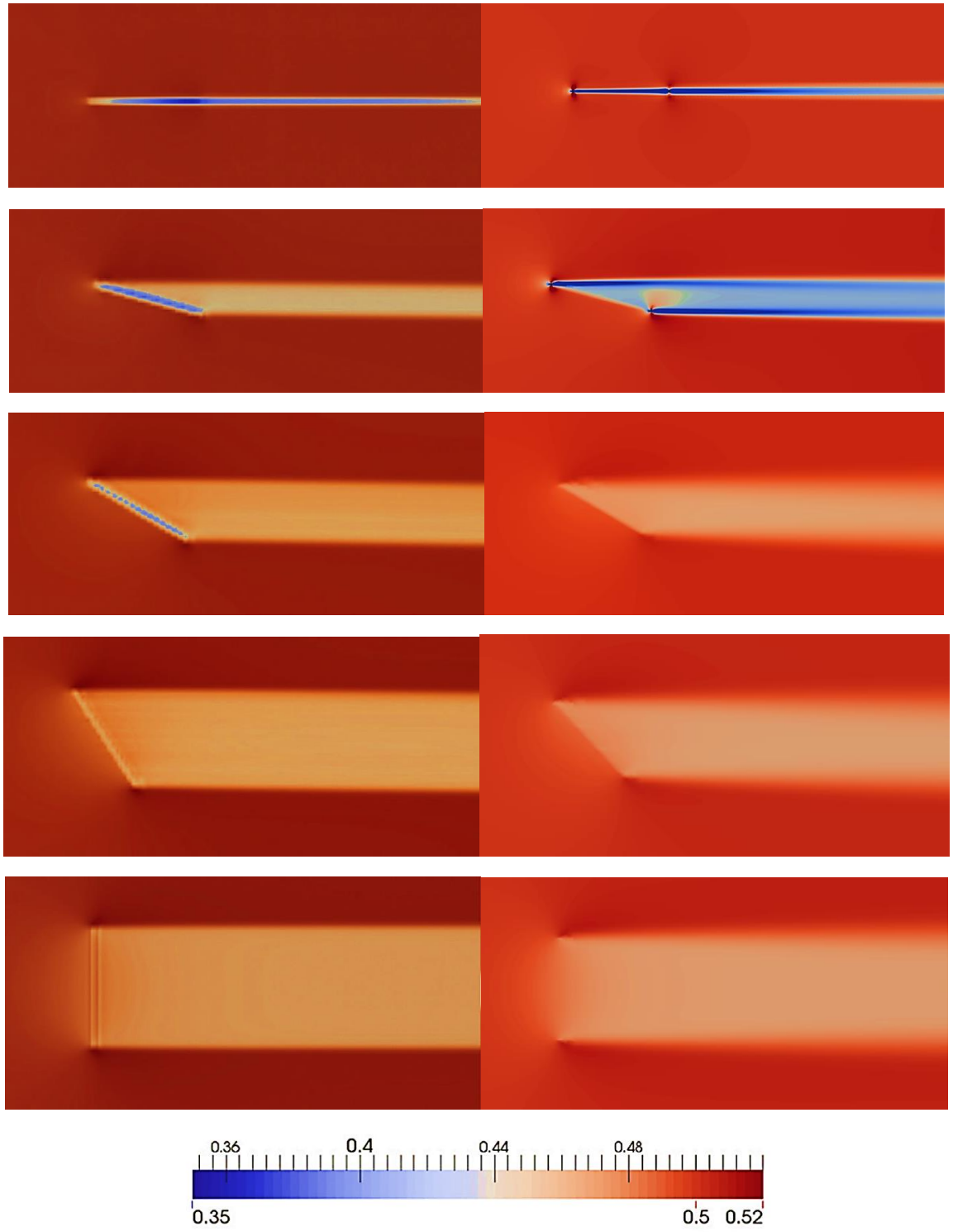

Figure 6 *Velocity contours through the centre of the net panel at different angles of attack for a flow speed of 0.5 m/s. Left are the CFD results of Chen and Christensen [4] and right are the marineFoam CFD results. Top to bottom are angles of attack 0º, 15º, 30º, 45º, 60º and 90º, respectively.*

The results from Figure 6 highlight a reasonable qualitative degree of concurrence between the two sets of CFD results. It should be noted that at shallow angles of attack such as 0° and

15° the cylindrical frame supporting the net may have an influence of the drag force and thus has been modelled in the CFD work of Patursson [2]. This was also carried out for the *marineFoam* study but was not included in the work of Chen and Christensen [4].

Figure 7 shows the drag force coefficients, C_d, lift force coefficients, C_l and velocity reduction factors U_r for the experimental data of Patursson [1], the CFD results of Patursson [2], the CFD results of Chen and Christensen [4] and the *marineFoam* CFD results. The velocity reduction factor is defined as:

$$U_r = \frac{U_o - U_{2.5}}{U_o} \tag{11}$$

where U_0 is the free-stream velocity and $U_{2.5}$ is the velocity 2.5 *m* downstream of the net panel.

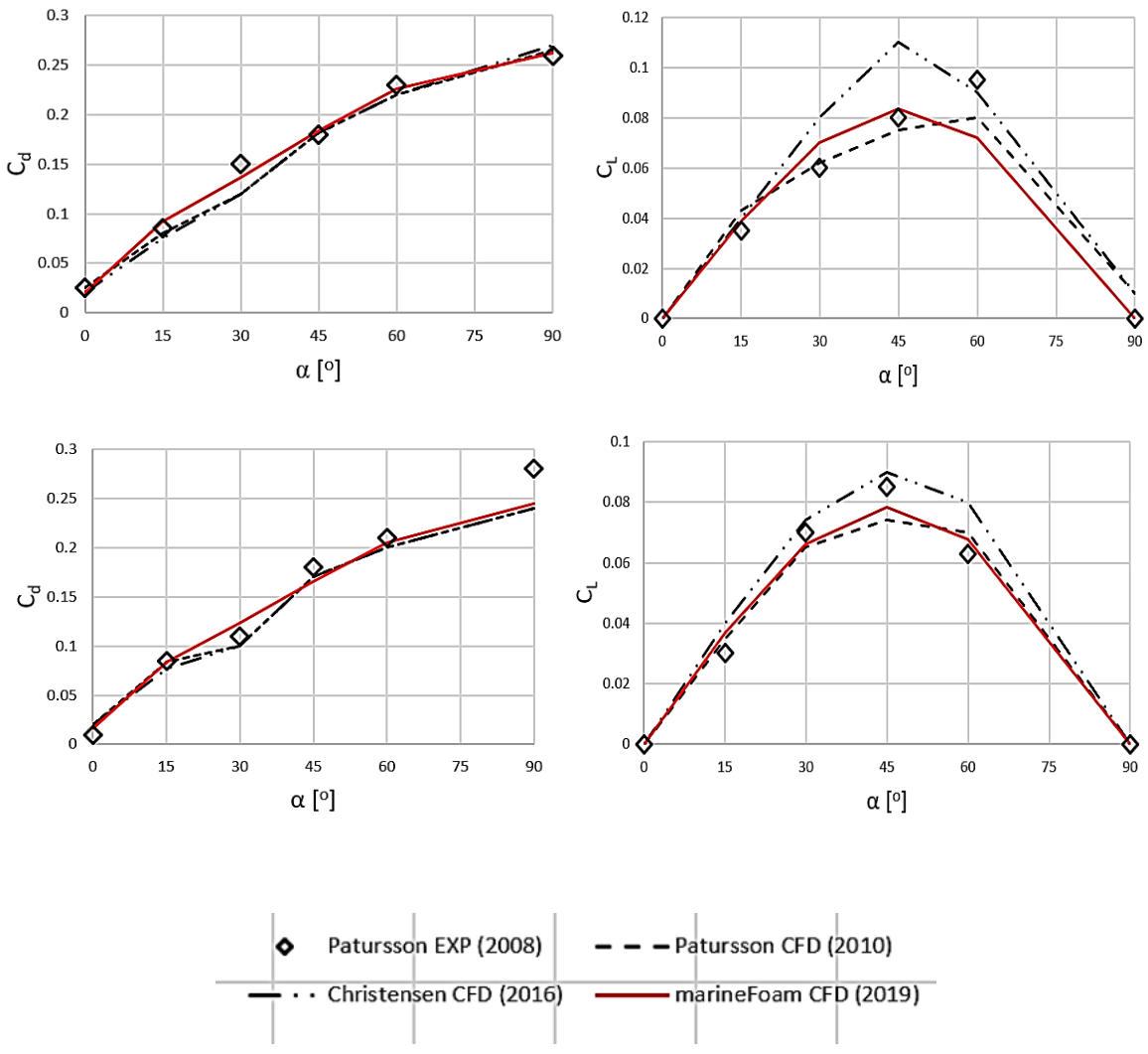

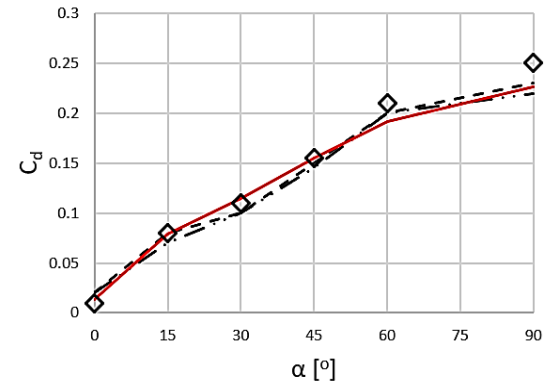
0.3
0.25
0.2
0.15
0.1
0.05
0
C_d
0
15
30
45
60
75
90
α [º]

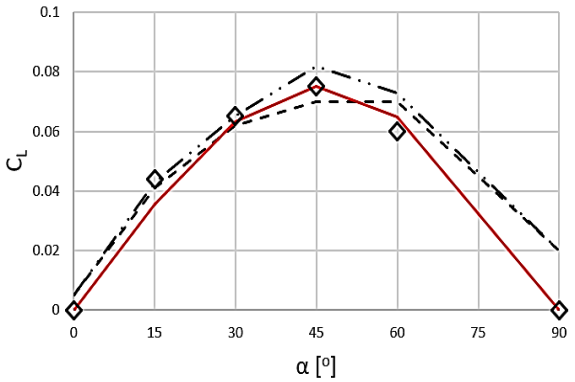
0.1
0.08
0.06
0.04
0.02
0
C_L
0
15
30
45
60
75
90
α [º]

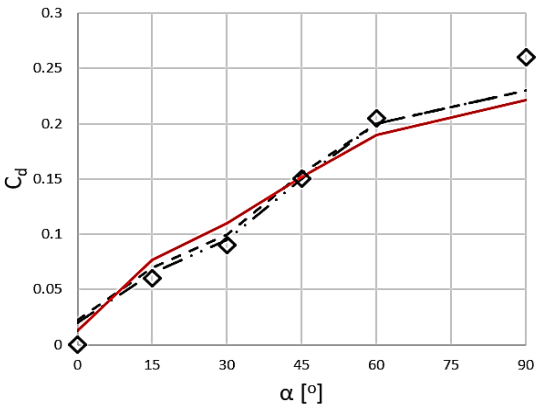
0.3
0.25
0.2
0.15
0.1
0.05
0
C_d
0
15
30
45
60
75
90
α [º]

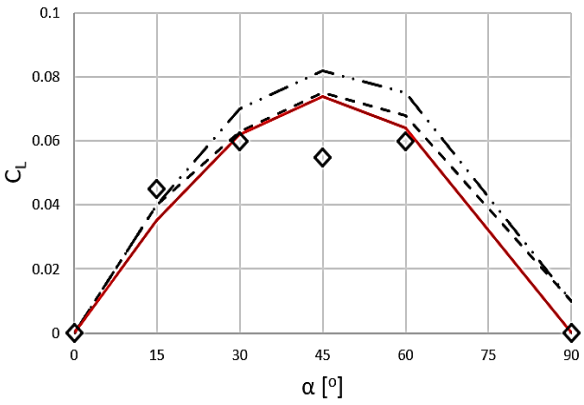
0.1
0.08
0.06
0.04
0.02
0
C_L
0
15
30
45
60
75
90
α [º]

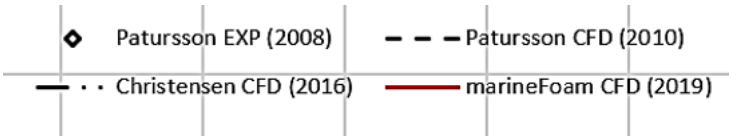
Patursson EXP (2008)
Patursson CFD (2010)
Christensen CFD (2016)
marineFoam CFD (2019)

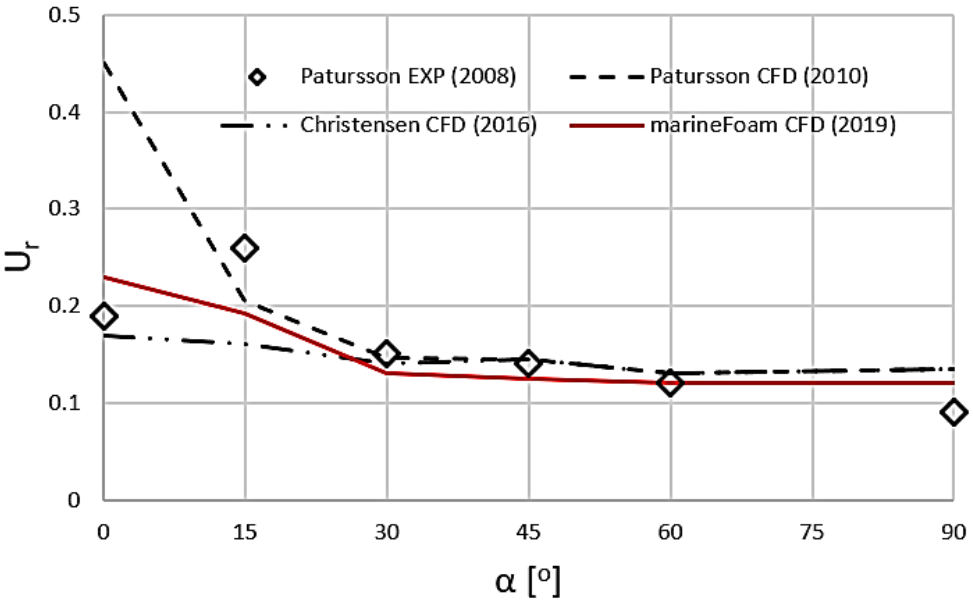
0.5
0.4
0.3
0.2
0.1
0
U_r
Patursson EXP (2008)
Patursson CFD (2010)
Christensen CFD (2016)
marineFoam CFD (2019)
0
15
30
45
60
75
90
α [°]

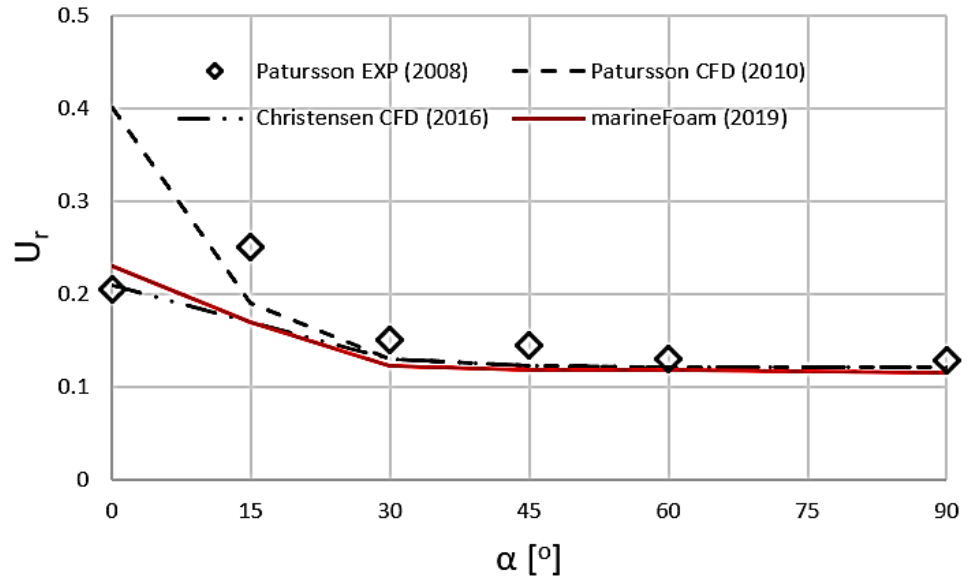
0.5
0.4
0.3
0.2
0.1
0
U_r
Patursson EXP (2008)
Patursson CFD (2010)
Christensen CFD (2016)
marineFoam (2019)
0
15
30
45
60
75
90
α [°]

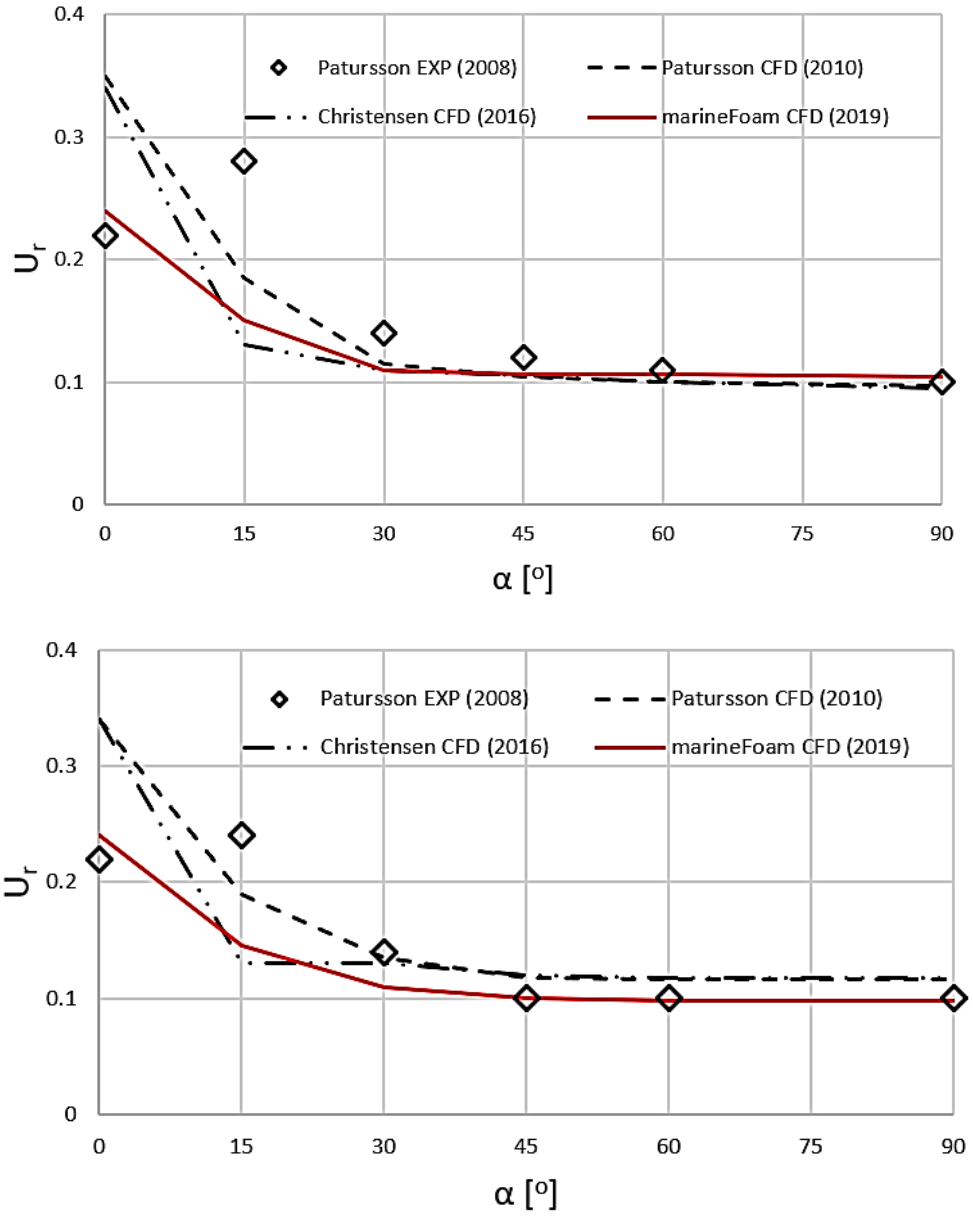

Figure 7 *Drag force coefficients, C_d, lift force coefficients, C_l and velocity reduction factors U_r for the experimental data of Patursson [1], the CFD results of Patursson [2], the CFD results of Chen and Christensen [4] and the marineFoam CFD results. Results top to bottom are for free stream velocities U_o =0.125 m/s, U_o =0.25 m/s, U_o =0.5 m/s, U_o =0.75 m/s, respectively.*

In general, the *marineFoam* results compare well with both the experimental and CFD results, in particular at shallow angles of attack where the inclusion of the cylindrical net frame appears to have an influence on the velocity reduction factors.

It is important to be able to model circular net cages as these appear to dominate the salmon farming industry. To this end, a CFD study of a circular cage was considered using *marineFoam*, with results compared with the experimental work of Zhan *et al* [9] and the CFD study of Chen and Christensen [4]. Figure 8 shows the experimental set-up for the circular cage study:

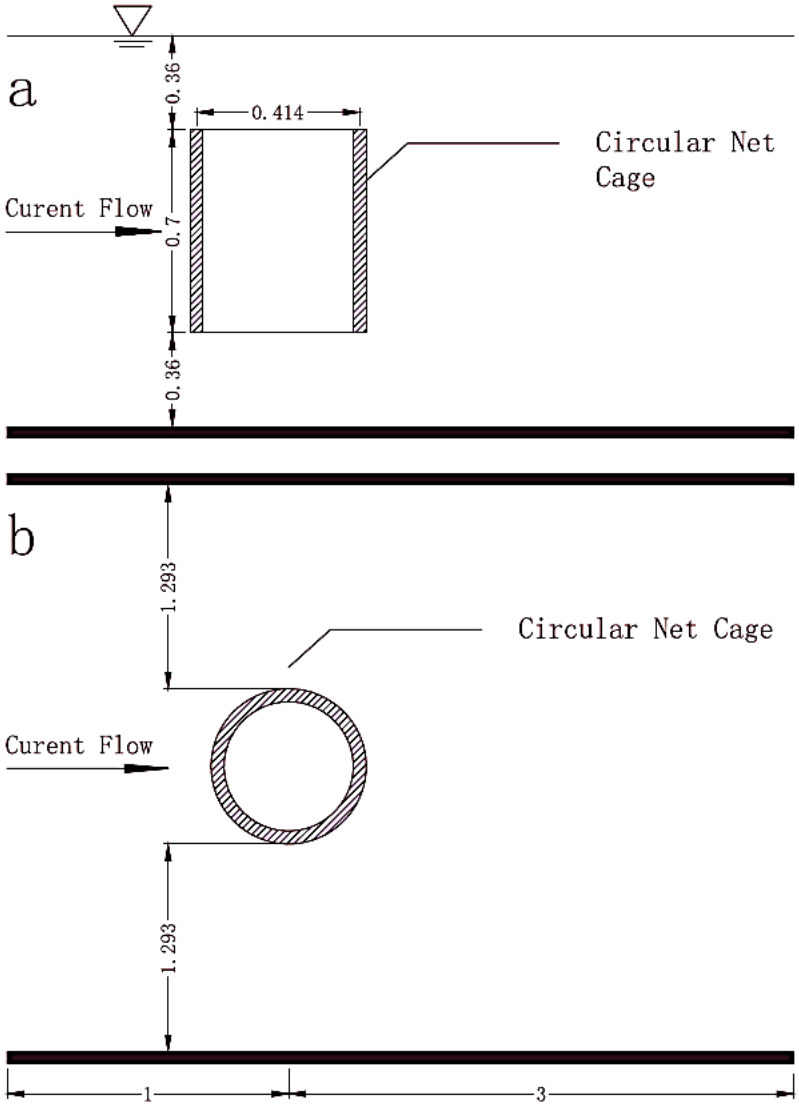

Figure 8 *Circular net configuration in the tow tank experiment of Zhan et al [9] (2006).*

In order to model the circular geometry, the work of Bi and Xu [5] has been followed in which the circular form of the cage is represented as an octagonal structure with planar sections at 0°, 22.5°, 45°, 67.5° and 90° with the corresponding Darcy and Forchheimer coefficients transformed using the matrix of equation 9. These coefficients come directly from the experimental work of Zhan *et al* [9] and are detailed in the paper of Chen and Christensen [4]. However, instead of using planar octagonal panels the *marineFoam* study has employed 16 arc segments of 22.5° as an alternative to the octagonal plane sections. The circular cage representation is shown in figure 9.

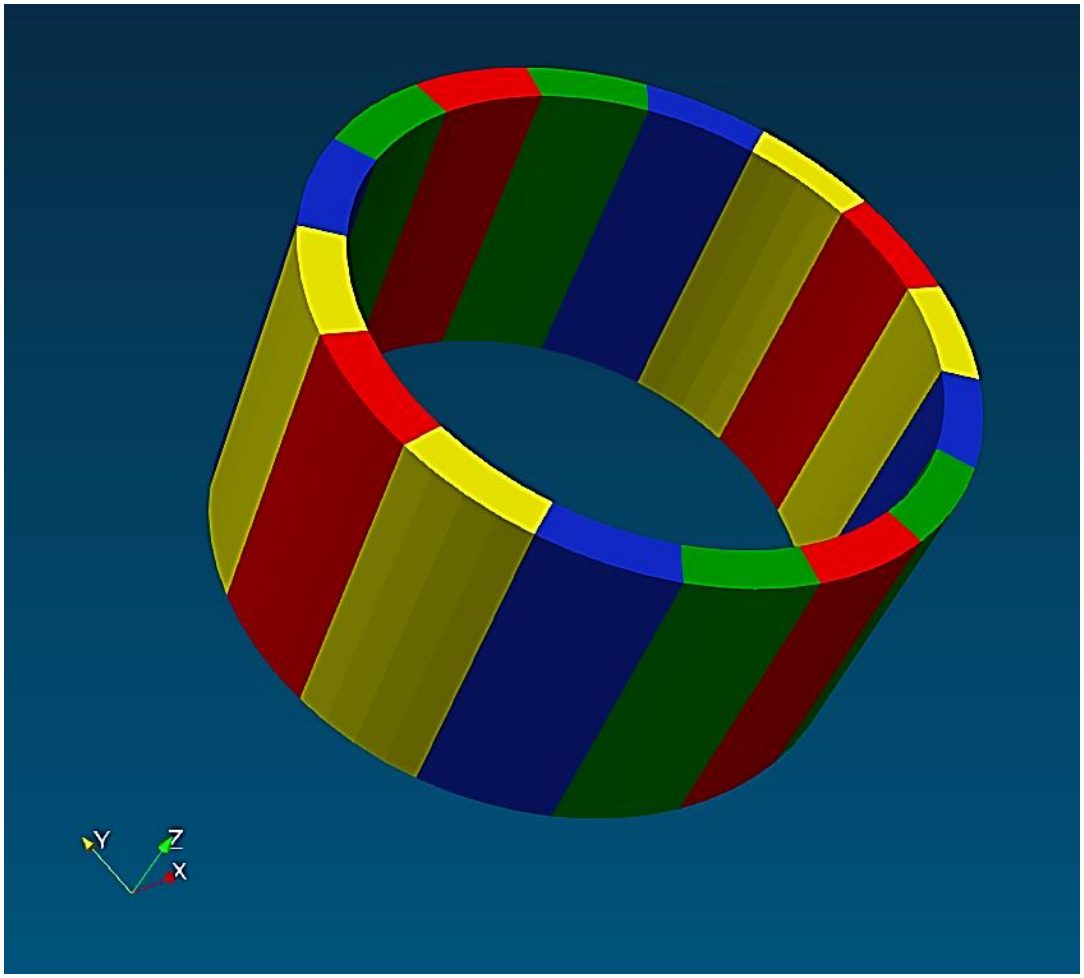

Figure 9 *Circular net configuration in marineFoam as 16 arc segments of 22.5°.*

Figure 10 shows the flow-field as velocity contours through the mid-section of the circular net at a flow speed of 0.5 m/s and a solidity ratio (net volume/free net volume) of S_n = 0.128.

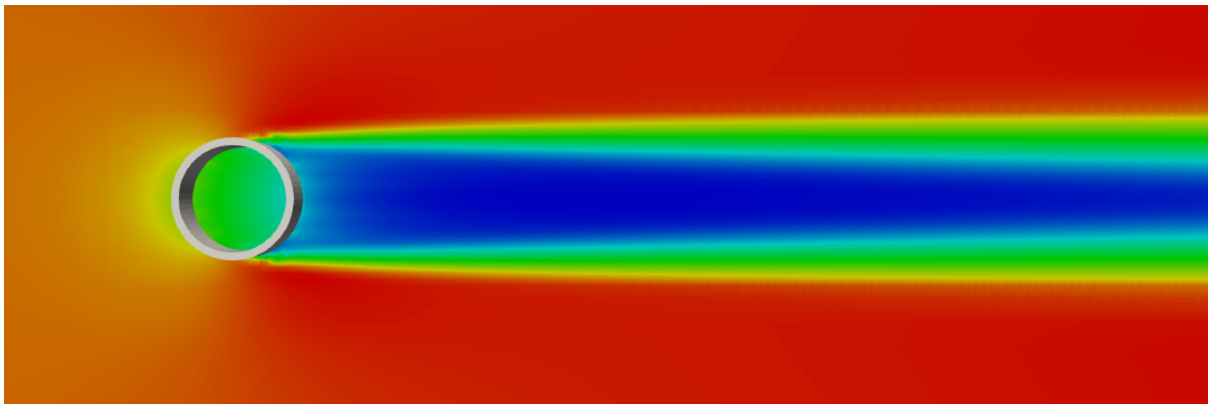

Figure 10 *marineFoam velocity contours for circular cage tow tank experiment of Zhan et al [9], (2006).*

Figure 11 shows the *marineFoam* predictions of drag force $F_{D,NET}$ [N] in comparison with the experimental work of Zhan et al [9] for two different solidity ratios, S_n = 0.128 and S_n = 0.215, respectively.

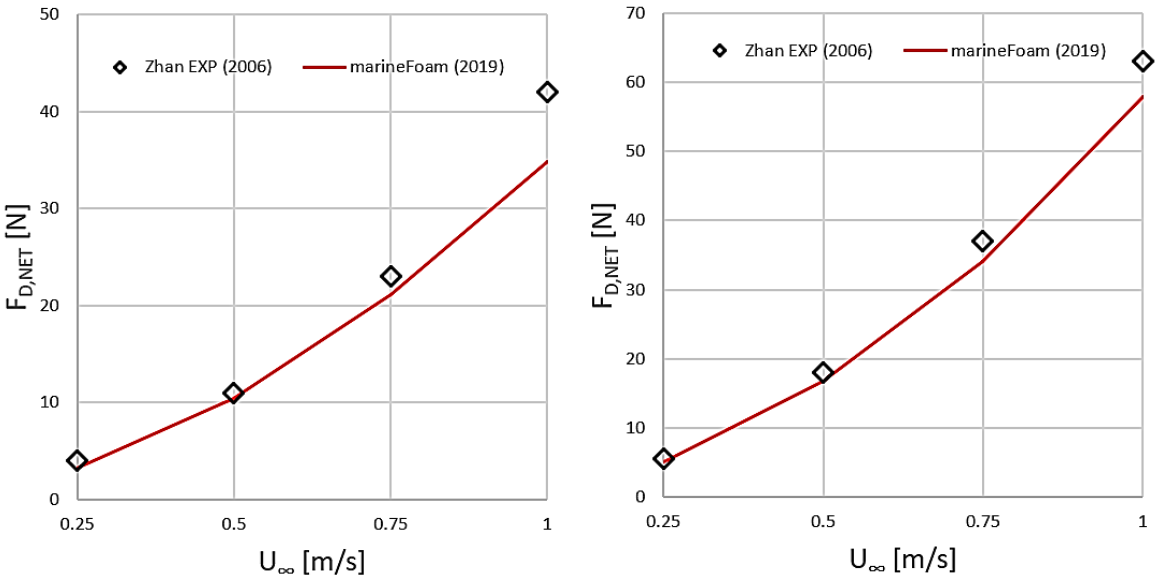

Figure 11 *marineFoam predictions of drag force for the circular cage tow tank experiment of Zhan et al [9], left S_n = 0.128, right, S_n = 0.215.*

In general, there is a satisfactory agreement between experimental and *marineFoam* results, particularly at lower velocities, implying that the arc segment method is a reasonable engineering approach for the representation of the circular cages.

4.1 Full scale fish farm model

The final test case considers the flow around a simulated full-scale salmon farm. Such a scenario was considered by Bi and Xu [5] and consists of an 8-cage farm, each of diameter 40 m with an equidistant spacing of 80 m between cage centres as shown in figure 12. The water depth is 50 m and the cage depth is 25 m. A constant flow speed of 0.1 m/s is set at the inlet and the inflow turbulence parameters k and epsilon were as prescribed in the paper of Winthereig-Rasmussen *et al* [3]. The lower boundary is set as a wall and the side boundaries were zero-gradient slip walls and a mesh size of ~1.5 M was employed as shown in figure 13. With a knowledge of the drag coefficient of C_d = 0.175 from the Bi and Xu paper [5] it was possible to extract the Darcy-Forchheimer porous resistance coefficients from a curve fit of equation 2 with pressure drop plotted as a function of flow speed. An example of the curve fit is shown in figure 14.

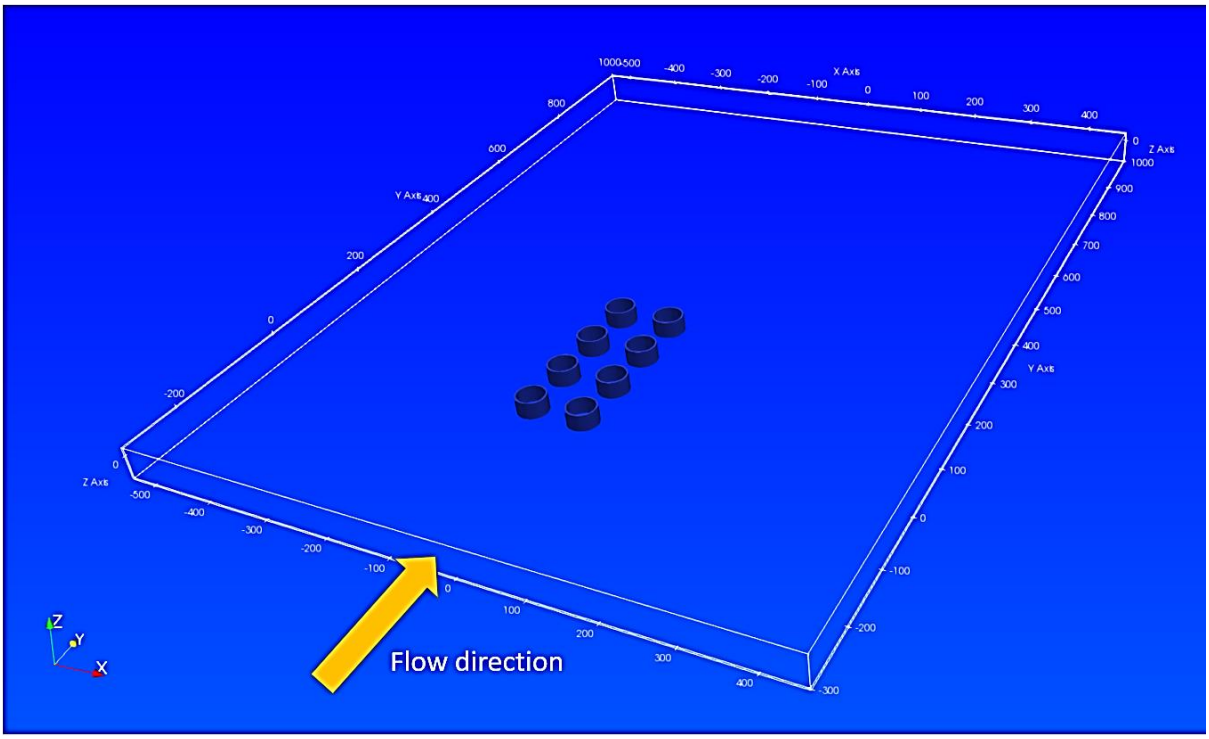

Figure 12 *Computational domain for full scale fish farm study.*

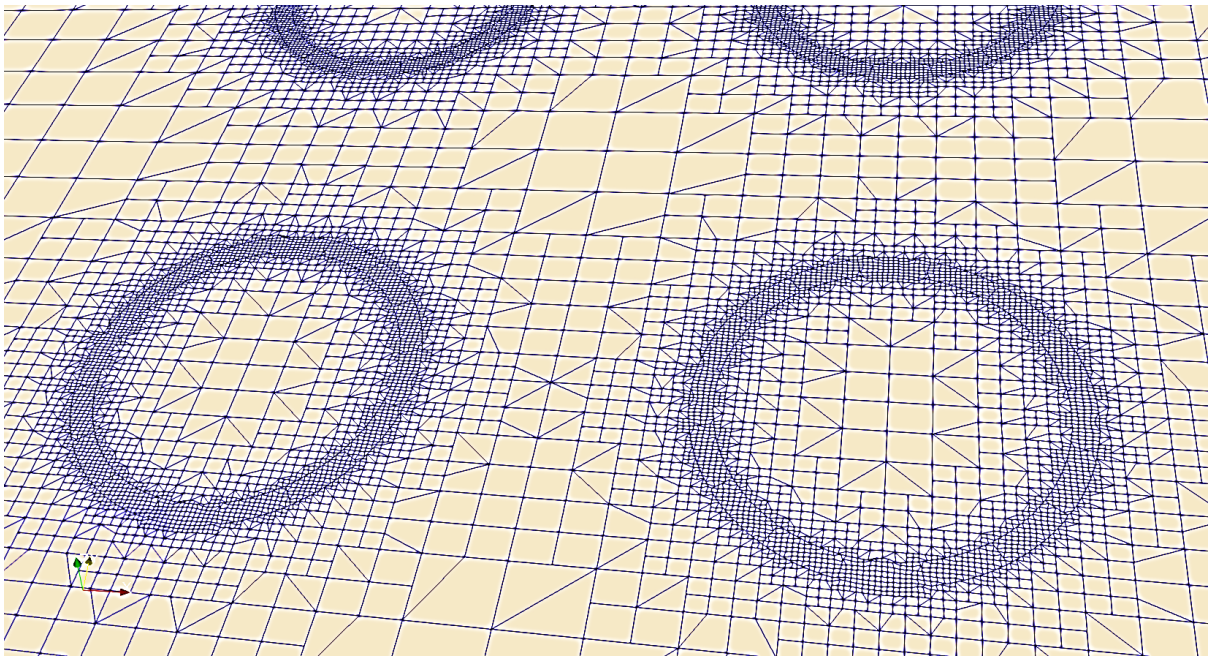

Figure 13 *Mesh distribution in region of salmon cages.*

Regression curve y=b*v+a*v²			
a	b		
87.4645161	0.00858065		
Parameter			
dx	3	m	Length of porous Zone
rho	999.975	kg/m³	Density of Fluid
mu	1.52E-03	Pa s	Dynamic viscosity of fluid
Coefficients (OpenFOAM definition - Adelaide paper)			
d	1.88172043	1/m²	Darcy coefficient
f	0.05831114	1/m	Forchheimer coefficient

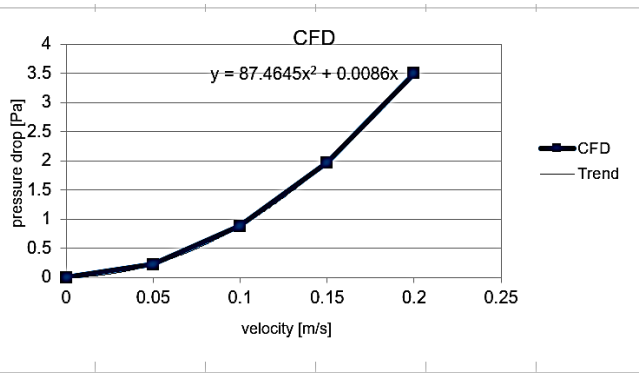

Figure 14 *Example of Excel regression curve for extraction of Darcy and Forchheimer porous resistance coefficients.*

Figure 15 shows the velocity contour plots along a section through the cage centres. There is a reasonable qualitative agreement between the *marineFoam* and Fluent (Bi and Xu [5]) plots. It is unclear as to the turbulence values employed by Bi and Xu and this can explain differences in the velocity distribution that appear evident.

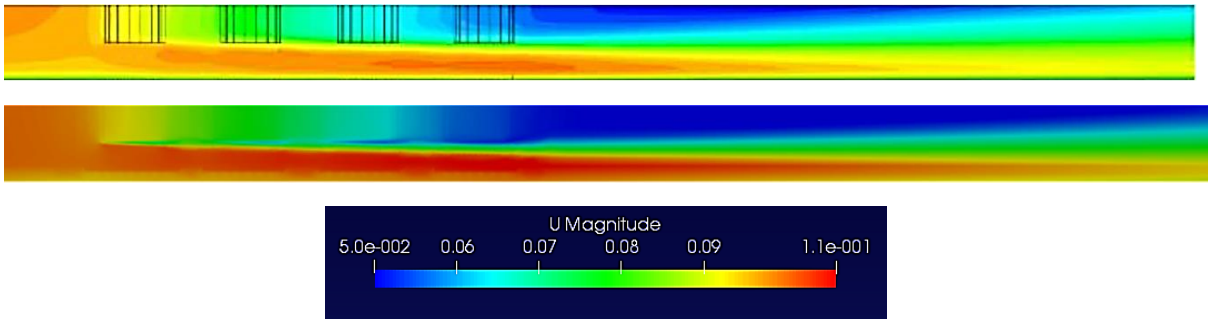

Figure 15 *Velocity contours through the centre-line of the cages – top Fluent, bottom marineFoam.*

The velocity magnitude through the centre-line of the salmon cages at a vertical position of half cage height is shown in figure 16. Both the *marineFoam* and Bi-Xu-Fluent plots compare well with the analytical results of Loland [6] with *marineFoam* capturing the analytical result particularly well at y/D = 3, where D is the cage diameter. Differences in the wake recovery velocities may be due to a lack of knowledge of the turbulence parameters employed by Bi and Xu and difference in meshing strategy.

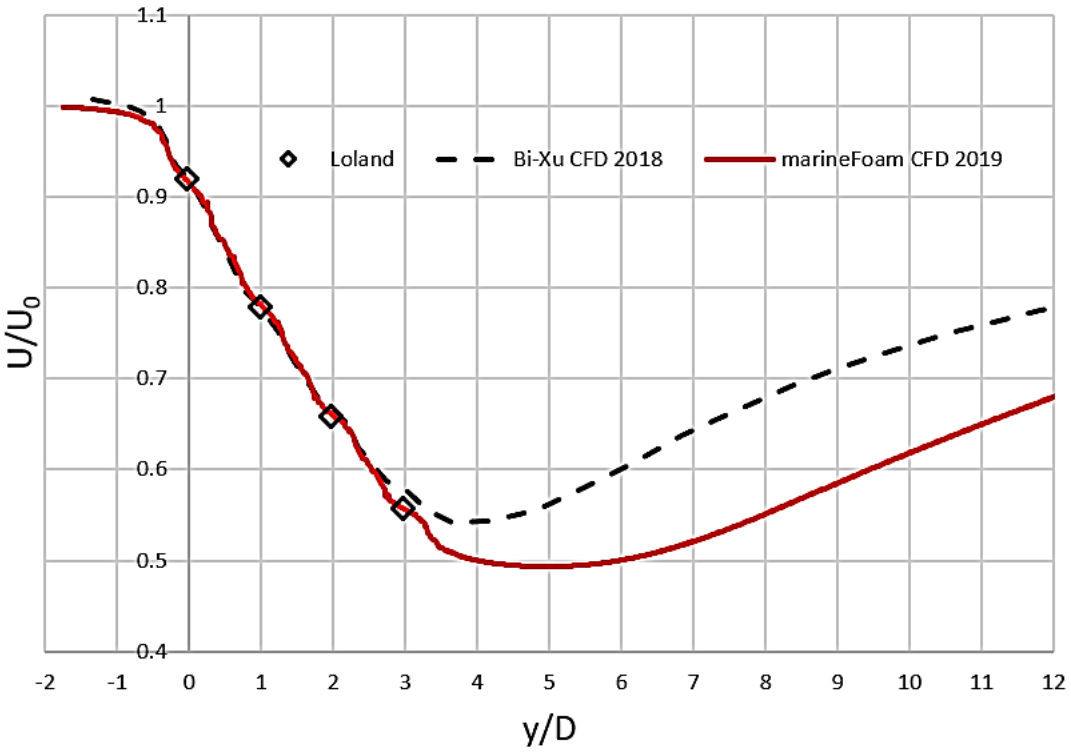

Figure 16 *Velocity reduction through the salmon cage centre-line at cage mid-height*

Finally, figure 17 shows the velocity contour distribution at the sea surface where it is evident that the cages have an important influence on the flow field wake for a significant distance downstream in the tidal flow.

5. Conclusions and Perspectives.

A new computational tool called *marineFoam* has been developed for the study of flow around and through salmon cages using porous media. The new model is designed to act as either a stand-alone simulator or to inform and improve current lower order models. *marineFoam* has been successfully validated and verified against analytical results, physical experiments and state-of-the-art numerical CFD codes. Future work could include studies of sea-bed particle resuspension, sea lice bath treatment chemical dispersion, the influence of caged salmon on flow blockage, particle tracking of farm-generated organic waste, deoxygenation effects in multi cage farms and the inclusion of complex topography in terms of bathymetry.

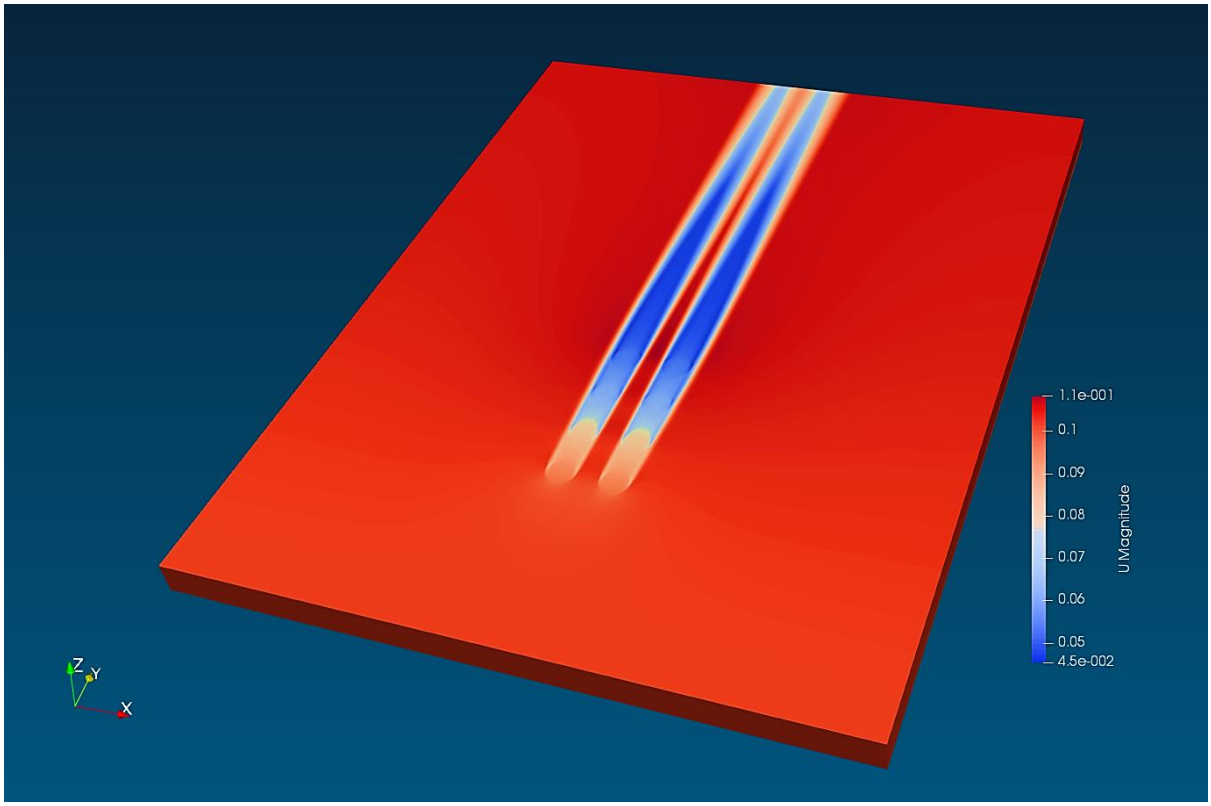

Figure 17 *marineFoam prediction of tidal speed at the sea surface.*

References

[1] Patursson, O., 2008, Flow through and around fish farming nets, PhD dissertation, Ocean Engineering, University of New Hampshire, Durham, NH 03824, USA.

[2] Patursson, O. *et al*, 2010, Development of a porous media model with application to flow through and around a net panel, *Ocean Engineering*, 37 (2-3), 314-324.

[3] Winthereig-Rasmussen, H. *et al*, 2016, Flow through fish farming sea cages: comparing computational fluid dynamics simulations with scaled and full-scale experimental data, *Ocean Engineering*, 124, 21-31.

[4] Chen, H. and Christensen, E., 2016, Investigations on the porous resistance coefficients for fishing net structures, *Journal of Fluids and Structures*, 65, 76-107.

[5] Bi, C. W. and Xu, T. J., 2018, Numerical Study on the Flow Field Around a Fish Farm in Tidal Current, *Turkish Journal of Fisheries and Aquatic Sciences*, 18, 705-716.

[6] Aarsnes, J., Rudi, H. and Loland, G., 1990, Current forces on cage net deflection, *Proc. ICE*, Glasgow, Thomas Telford, 137-152.

[7] https://www.mts-cfd.com/ Accessed 5th February 2019.

[8] Bejan, A., *Convection Heat Transfer*, John Wiley and Sons, 1984.

[9] Zhan, *et al*., 2006, Analytical and experimental investigation of drag on nets of fish cages, Aquaculture Engineering, 35 (1), 91-101.